pH-sensitive behavior of the PS-b-PDMAEMA copolymer at the air - water interface

Louis Bondaz, Fabrice Cousin, François Muller, Nadège Pantoustier, Patrick Perrin, Alessandra Luchini, Michel Goldmann, Philippe Fontaine

pH-sensitive behavior of the PS-b-PDMAEMA copolymer at the air - water interface

Louis Bondaz [a,b,c], Fabrice Cousin [d], François Muller [b,d], Nadège Pantoustier [e], Patrick Perrin [e], Alessandra Luchini [f,1], Michel Goldmann [a,c,g], Philippe Fontaine [a,c,*]

[a] Synchrotron SOLEIL, L'Orme des Merisiers, BP 48, Saint-Aubin, 91192, Gif sur Yvette, France
[b] Nanosciences and Nanotechnologies group, ECE Paris Ecole d'Ingénieurs, 75015 Paris, France and INSEEC U Research Center, 75015, Paris, France
[c] Sorbonne Université, UPMC Université Paris 06, CNRS-UMR 7588, Institut des NanoSciences de Paris, 4 place Jussieu, F-75005, Paris, France
[d] Université Paris-Saclay, Laboratoire Léon Brillouin, CEA-CNRS, CEA Saclay, 91191, Gif-sur-Yvette, France
[e] Soft Matter Sciences and Engineering, ESPCI Paris, PSL University, Sorbonne Université, CNRS, 75005, Paris, France
[f] Institut Laue-Langevin - 71 avenue des Martyrs, CS 20156, 38042, GRENOBLE Cedex 9, France
[g] Faculté des Sciences Fondamentales et Biomédicales, Université de Paris, 45 rue des Saints Pères, 75006, Paris, France

ARTICLE INFO

Keywords:
Amphiphilic diblock copolymers
Polyelectrolytes
Neutron reflectivity
Polymer at the air/water interface
Polyelectrolyte brush
Scaling laws

ABSTRACT

We investigated the behavior of a pH-responsive polystyrene-*b*-poly(2-dimethylamino)ethyl methacrylate (PS-*b*-PDMAEMA) diblock copolymer at the air/water interface. We synthetized different copolymers with a small hydrophobic PS block of constant length attached to polyelectrolyte PDMAEMA blocks of various lengths. We demonstrate that a Langmuir monolayer is formed with the hydrophobic collapsed PS block anchoring the hydrophilic polyelectrolyte at the interface. By combining macroscopic surface pressure measurements and specular neutron reflectivity, we studied the monolayers as a function of surface density σ and pH of the subphase. At pH = 2, the PDMAEMA is fully charged and the system at high σ behaves as a polyelectrolyte brush with chains protruding in water with a gaussian profile. At pH = 10 where the PDMAEMA is neutral, the system exhibits a phase transition between the pancake configuration to the brush configuration, with a threshold that depends on the PDMAEMA chain length, in agreement with theoretical predicted scaling laws.

1. Introduction

Poly(2-dimethylamino)ethyl methacrylate (PDMAEMA) is a weak poly-base which is water soluble at neutral and acidic pH [1]. It exhibits a pKa value between 6.5 and 7 [1] and a varying hydrophobicity with temperature due to disruption of hydrogen bond between DMAEMA and water [2], which give it a large potential to design stimuli-responsive systems. Associated with a neutral hydrophobic polystyrene (PS) in a copolymer (PS-PDMAEMA), it was indeed used to produce stimuli-responsive emulsions for which the change from water/oil to oil/water emulsions can be triggered reversibly using temperature, ionic strength or pH [1,2]. PDMAEMA copolymers were also used to obtain pH reversible micellization [3], controlled drug release [4], pH and thermo-responsive hydrogels [5].

Recently, we use PS-*b*-PDMAEMA micelles in solution as nano-molds for gold nanoparticles synthesis through the reduction by x-ray radiolysis of $AuCl_4^-$ ions trapped in the PDMAEMA chains [6]. We aim now to apply such a strategy on planar brushes of PDMAEMA chains as mold to form metal thin layers by the surface x-ray radiolysis technique [7,8]. Indeed, the possibility to vary independently the grafting density σ and the responsiveness of the PDMAEMA block through the pH or ionic strength, would allow to obtain rich phase behavior and therefore various morphologies for the molds. A first approach to design PDMAEMA brushes would be to chemically graft the polymer chains onto a solid surface by the "grafting-to" technique, the "grafting-from" technique or the physical adsorption on a hydrophobic substrate of a copolymer with one anchoring hydrophobic block [9]. However, these techniques do not allows to vary σ without making a new synthesis [10]. A better approach is then to use PS-*b*-PDMAEMA copolymers spread as a monolayer at the air/water interface, with the hydrophobic PS block, frozen at ambient temperature, enabling the anchoring of the water soluble PDMAEMA block at the interface. Indeed, the design of brushes

* Corresponding author. Synchrotron SOLEIL, L'Orme des Merisiers, BP 48, Saint-Aubin, 91192, Gif sur Yvette, France.
E-mail address: philippe.fontaine@synchrotron-soleil.fr (P. Fontaine).
[1] Present Addresses: Niels Bohr Institute, University of Copenhagen, Universitetsparken 5, 2100, Copenhagen, Denmark.

at the air-water interface with hydrophobic/hydrophilic diblock copolymers offers the possibility to adjust σ by varying the interface area accessible to the macromolecules [10–22]. The hydrophilic/hydrophobic balance governs the ability of the copolymer to spread at the air-water interface and to form a Langmuir monolayer. The area per chain of the monolayer, i.e. 1/σ, can then be continuously varied on a Langmuir trough to set the polymer density at the interface to a target value.

The wide range of applications of polyelectrolyte brushes [23–25] have motivated numerous theoretical [11,23,24,26,27] and experimental studies [10,12–18,28–30] aiming at describing their behavior when they are tethered at an interface with a solvent. Several predictions were reported describing the influence on their conformation of the relevant physico-chemical parameters of the system, such as the solvent quality, the grafting density σ, the ionic strength, the polymer molecular mass and the linear charge density of the chain [11,23,31–33]. The typical description of the polyelectrolyte layer upon increase of σ is a conformational change from a mushroom or pancake configuration, depending on the respective affinity of the monomers with the solvent and the interface, to a brush regime where the chains are stretched in the solvent. Indeed, at low σ, the chains are separated from each other and weakly interacting if electrostatic interactions are sufficiently screened. In this situation, the chains can adopt a mushroom configuration in a good solvent or a pancake configuration if the adsorption on the surface is more energetically favorable [23]. When increasing σ, inter-chain interactions may increase and induce a transition to a brush conformation where the chains protrude in the liquid phase.

In this paper, we present a comprehensive study of the behavior of the polystyrene-*b*-poly(2-dimethylamino)ethyl methacrylate (PS-*b*-PDMAEMA) amphiphilic copolymer at the air-water interface in various physicochemical conditions by probing the influence of σ, ionic strength, PDMAEMA block length and pH. We focus on two characteristic subphases: an acidic one (pH = 2) where the PDMAEMA block is fully charged and an alkaline one (pH = 10) where the PDMAEMA block is fully neutral. We characterized the samples by combining 2D thermodynamical macroscopic measurements with structural determination at the molecular scale by means of specular neutron reflectivity measurements [34]. This study will serve as a foundation for the further use of PS-*b*-PDMAEMA at the air/water interface for dedicated applications.

2. Experimental

2.1. PS-b-PDMAEMA synthesis

The diblock copolymers consist of a polystyrene (PS) block and a poly-2-(dimethylamino)ethyl methacrylate (PDMAEMA) block. These PS_x-*b*-$PDMAEMA_y$ amphiphilic copolymers were synthesized by atom transfer radical polymerization using the "halogen exchange" method [1,2,6]. Details of the synthesis procedure can be found in our previous paper [6]. The number (M_n) average molar masses, as well as the dispersity ($Đ = M_w/M_n$), of the synthesized polymers were determined by size exclusion chromatography (SEC) in THF containing 2 wt% trimethylamine at 40 °C with a flow rate of 1 mL min^{-1} using a Viscotek SEC system (Viscotek VE 2001 GPC Solvent - GPC MAX - Sample Module and TDA 302 triple detector array) equipped with two PLgel 5 μm Mixed-C columns (7.5 × 300 mm). 100 μL of polymer solution was injected at a concentration of 4 mg mL^{-1} after filtration through a 0.22 μm pore size membrane. The 'absolute' molar masses were determined by the three inline detectors (refractometer, viscometer, and light scattering) relying upon a calibration based on polystyrene standard. All measurements were performed as triplicates.

^{1}H NMR spectroscopy: spectra were recorded with a Bruker 400 MHz spectrometer in 5 mm diameter tubes, using deuterated chloroform at room temperature, and were used to determine precise composition of each synthesized copolymer. Four copolymers (based on PS_x-b-$PDMAEMA_y$) were synthesized for this study and their macromolecular characteristics are gathered in Table 1. x and y indexes on PS_x-b-$PDMAEMA_y$ block copolymers represent the average number of monomer units of styrene (N_S) and 2-(dimethylamino)ethyl methacrylate (N_{DMAEMA}) respectively. Three of them have the same PS block length (x = 36 monomer units) with 3 different lengths for the $PDMAEMA_y$ block (y = 87, 110, 167). In addition, the PS^d_{30}-*b*-$PDMAEMA_{100}$ copolymer was synthetized with a deuterated PS block in order to use the contrast variation technique for the neutron reflectivity experiments [6]. The hydrogenated polymers are PS_{36}-*b*-$PSMAEMA_{87}$, PS_{36}-*b*-$PSMAEMA_{110}$, PS_{36}-*b*-$PSMAEMA_{167}$ and the deuterated one is PS^d_{30}-*b*-$PDMAEMA_{100}$.

2.2. Langmuir monolayer formation and thermodynamical measurement

The synthesized copolymers are fully soluble in chloroform, which is classically used as spreading solvent to form Langmuir monolayers since it is non-miscible with water and highly volatile [35]. Spreading solutions are made of a copolymer concentration 10^{-4} mol L^{-1} dispersed in chloroform (VWR France, Normapur grade). Aqueous subphases were obtained using ultra-pure water (Milli-Q water, 18.2 MΩ cm). pH of the subphase was adjusted by adding hydrochloric acid (HCl, VWR France, Normapur grade) to obtain the subphase at pH = 2 and sodium hydroxide (NaOH, VWR France, Normapur grade) for the subphase at pH = 10.

The copolymer films were probed on a computer-interfaced Langmuir trough equipped with a Wilhelmy balance (R&K GmbH, Potsdam, Germany) to measure the surface pressure (π) with an accuracy of ±0.1 mN m^{-1}. A connected thermostat kept the temperature at 18 °C with a precision of ±0.1 °C. The solutions were spread carefully from a microsyringe (Hamilton, Switzerland) onto the aqueous subphase. The chloroform was allowed to evaporate for 10 min before starting compression. The films were compressed using a moveable barrier with a velocity of 12 cm^2 min^{-1}, until the compression limit was reached. Afterwards, the films were immediately expanded in order to determine the reproducibility of the isotherm or an eventual hysteresis. It does not reveal significant hysteresis and thus loss of material from the interface nor slow-kinetic relaxations. All isotherms were measured at least twice for reproducibility.

We also verified that the thermodynamical measurements of surface pressure, π vs. area per chain were almost similar for both PS_{36}-*b*-$PSMAEMA_{110}$ and PS^d_{30}-*b*-$PDMAEMA_{100}$ copolymers, whatever the content of D_2O in the aqueous subphase [36].

2.3. Specular neutron reflectivity (SNR) measurements

Reflectivity measurements were performed on the time of flight reflectometer FIGARO at the Institut Laue Langevin (ILL, Grenoble, France) [37]. Each reflectivity curve was collected in the q_z-range 0.06 nm^{-1}- 2 nm^{-1} with 1-h acquisition time at two incident angles ($\alpha_1 = 0.62°$, $\alpha_2 = 3.8°$). Incoherent scattering was measured for each

Table 1
Macromolecular characteristics of the PS_x-b-$PDMAEMA_y$ copolymer.

Block copolymer PS_x-b-$PDMAEMA_y$ [b]	M_n [a] (g. mol^{-1})	Đ	N_S/ N_{DMAEMA} [b]	N_S/ N [b]	N_{DMAEMA}/ N [b]
PS_{D30}-b-$PDMAEMA_{100}$	19000	1.14	0.30	0.23	0.77
PS_{36}-b-$PDMAEMA_{87}$	17500	1.09	0.41	0.30	0.70
PS_{36}-b-$PDMAEMA_{110}$	21100	1.24	0.32	0.25	0.75
PS_{36}-b-$PDMAEMA_{165}$	29600	1.3	0.22	0.18	0.82
PS_{36}	3750	1.08	–	–	–

[a] Number average molar mass (M_n) as determined by triple detection-SEC analysis in THF containing 2% triethylamine.

[b] x and y indexes on PS_x-b-$PDMAEMA_y$ being the average number of monomer units of each type (N_S and N_{DMAEMA} for styrene and 2-(dimethylamino)ethyl methacrylate respectively, N represents the total number of monomer units, N_S + N_{DMAEMA}) as determined by ^{1}H NMR analysis.

sample out of the specular plane and was subtracted from every curve.

We used the contrast variation technique to probe selectively the structure of each block within the monolayer. This prompted us to use the PS^{d}_{30}-*b*-$PDMAEMA_{100}$, since the scattering length density (SLD) of PS^{d} block ($6.5.10^{-4}$ nm^{-2}) is very different from the one of a PDMAEMA melt, estimated as 0.9 10^{-4} nm^{-2}. Hence neutron reflectivity measurements were performed on two different H_2O/D_2O subphases to match selectively the scattering from each block: 100% D_2O, whose SLD ($6.39.10^{-4}$ nm^2) matches almost the PS_d's SLD, and only reveal the structure of the PDMAEMA and 18% D_2O/82% H_2O (SLD of $0.7.10^{-4}$ nm^{-2}) to probe the structure of the PS^{d} block. We performed SNR measurements at different representative measurement points of the whole π-A isotherms. In the following, we refer to these points either by their surface pressure or to their area per chain at large surface area when the surface pressure that is close to zero. The collected data were analyzed with the GenX software [38]. This software allowed to fit the same structural model to the data collected for the two different subphases.

3. Results and discussion

3.1. Acidic subphase

Surface pressure *vs.* area per chain isotherms of PS_{36}-*b*-$PDMAEMA_N$ on acidic (pH = 2) aqueous subphase are reported on Fig. 1. The evolution of surface pressure along the compression is characterized by a near-zero surface pressure plateau at low surface density (high area per chain), followed by an increase of surface pressure with a lift-off area around 30 nm^2 per PS-*b*-PDMAEMA molecule, and a limit area near 10 nm^2 per chain (interception between the x-axis and the asymptote line of the curve at high pressure). Only a small shift to high area per chain with increasing polyelectrolyte block length of the copolymer is observed. The compressibility of the phase corresponding to the non-zero surface pressure region is about 15 m N^{-1} (determined from the numerical derivative of the compression π-A isotherm). The collapse is not reached at the smallest area per chain probed (5 nm^2) and occurs at surface pressures larger than 42 mN m^{-1}.

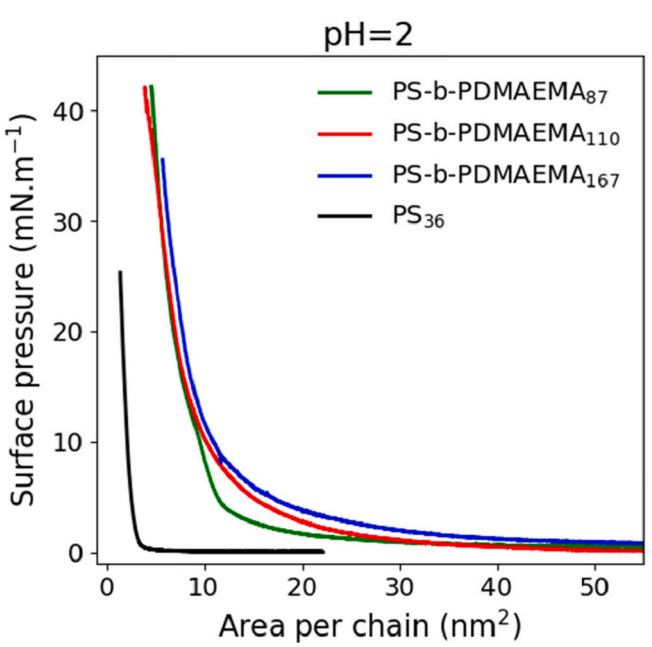

Fig. 1. Surface pressure vs. area per chain isotherm of polystyrene homopolymer (PS_{35}) on pure water, PS_{36}-b-$PDMAEMA_N$ with N = 87, 110, and 167 on pH = 2 water subphase at 18 °C. The x-axis is the area per PS-b-PDMAEMA or PS molecule.

A comparison between the isotherms collected for the copolymer on the acidic subphase with the isotherm collected for a polystyrene homopolymer PS_{35} is reported in Fig. 1. The characterized PS homopolymer, considered as glassy below T_g, has a molar mass almost identical to the one of the PS block in the PS_{36}-*b*-$PDMAEMA_{110}$. The isotherm of the PS monolayer was collected to determine if the polystyrene block influences the limit area of the surface pressure compression in the isotherms of PS_{36}-*b*-$PDMAEMA_{110}$. The compression isotherm for the PS_{35} homopolymer exhibits a zero-surface pressure plateau ending by a lift-off at 4 nm^2 per molecule. The limit area is around 3 nm^2 per molecule, much smaller than those of the PS_{36}-*b*-$PDMAEMA_{110}$ copolymer, and the collapse pressure is around 25 mN m^{-1} leading to a compressibility of about 10 m N^{-1}. Therefore, we conclude that the PS block does not set the limit areas of the copolymers isotherms.

The influence of the ionic strength of the subphase when PDMAEMA blocks are charged was tested and the corresponding π-A isotherms at pH = 2 are presented in Fig. 2. Increasing the ionic strength with a monovalent salt (KCl) does not change significantly the curves except a slight decrease of the lift-off values. Such lift-off corresponds to the point where electrostatic repulsions between PDMEAMA chains become prominent. Its value slightly below 30 nm^2 corresponds to the point where the mean distance between chains is of the order of the Debye Length λ_D, equal to 3 nm at pH = 2 when the ionic strength of the subphase is 10 mmol L^{-1}. For such ionic strength, electrostatic interactions between chains are then already largely screened which explains why the isotherm is almost not affected when the ionic strength increases from 10 mmol L^{-1} up to 110 mmol L^{-1} (Fig. 2). One only observes a slight shift of the curve towards lower area per chain due to screening of interactions.

Fig. 3 shows the specular neutron reflectivity curves of the monolayer of PS^{d}_{30}-*b*-$PDMAEMA_{100}$ at pH = 2 and various surface pressures, for both 82%H_2O/18%D_2O (A) and 100%D_2O (B) subphases. These curves are displayed in the Fresnel representation $R(q_z)q_z^4$ versus q_z in order to get rid from the intrinsic q_z^{-4} decay of the bare air/water interface far from the critical scattering vector q_c. The reflectivity curves of the bare liquid subphases were analyzed with the model including a simple rough interface between two media. One obtains in both cases a roughness around 0.2 nm in agreement with the expected value for the air/water interface. The fits of the bare subphases enable to determine experimentally their SLD as 0.58 10^{-4} nm^{-2} for 82%H_2O/18%D_2O (theoretical SLD value 0.7 10^{-4} nm^{-2}) and 6.31 10^{-4} nm^{-2} for 100%

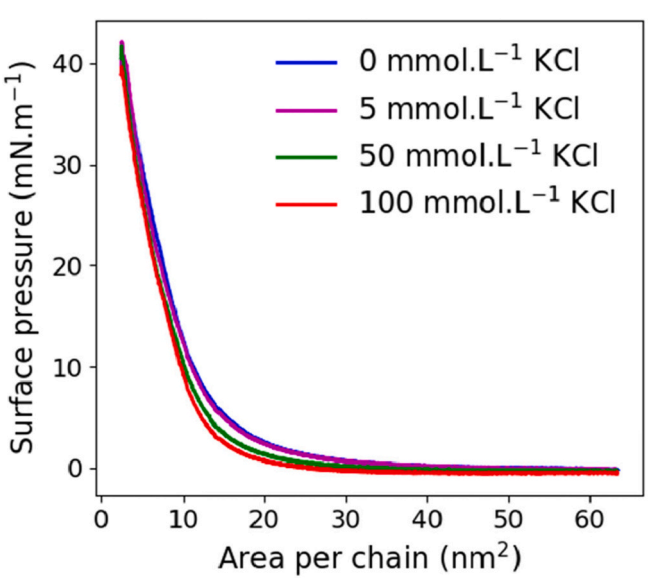

Fig. 2. Effect of KCl salt dissolved in the water subphase on the surface pressure – area per chain isotherm of PS_{36}-b-$PDMAEMA_{110}$ copolymer.

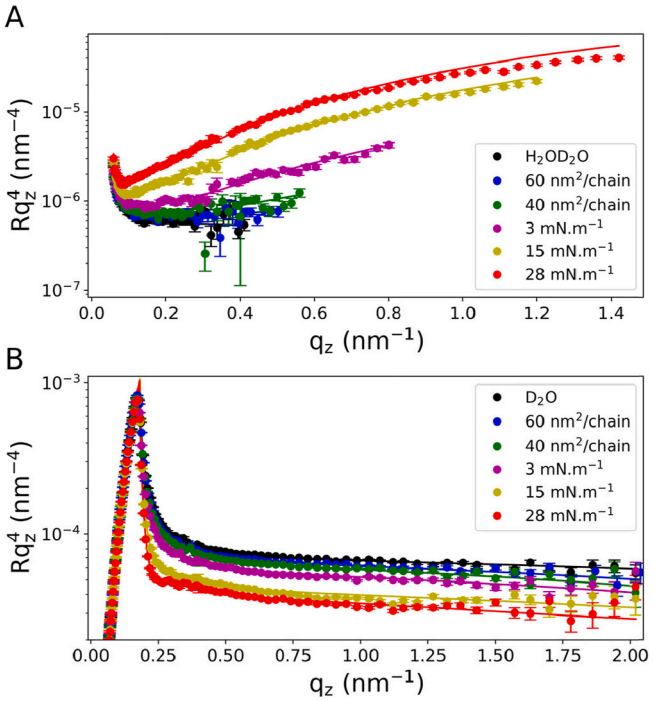

Fig. 3. Neutron reflectometry spectra in Rq_z^4 representation PS^d_{30}-b-$PDMAEMA_{100}$ deposited on acidic (pH = 2) 82%H_2O/18%D_2O subphase (A) and 100%D_2O subphase (B). Experimental data are represented as dots, while lines are used to represent the adjustment with a multilayer model (see text).

D_2O (theoretical SLD value 6.39 10^{-4} nm^{-2}). The discrepancy of the SLD deduced from the analysis of the reflectivity curves and the nominal value calculated from the H_2O/D_2O content in the subphase results from the introduction of HCl to adjust the pH of the subphases. The measured SLD values for the subphases were considered as constants during the analysis of the data collected for the copolymer layer.

The evolution of the SNR curves on acidic 82%H_2O/18%D_2O subphase as function of the applied surface pressure with respect to the curve for the bare subphase can be mainly ascribed to the PS block (Fig. 3-A). At large area per chain (60 nm^2), the SNR curve has a larger intensity than the bare subphase, revealing the presence on the surface of molecular species with a larger SLD compared to the one of the subphase. Upon compression of the monolayer, an oscillation arises, which gets more and more enhanced and shifts slightly towards lower q_z with increasing surface pressure. This suggests the formation of a small layer with a low roughness. The increasing upon compression of the SLD of this layer, formed by PS blocks and air, indicates that the volume fraction of PS increases within this layer.

For the 100%D_2O subphase which matches the PS (Fig. 3-B), the collected curve at 60 nm^2 per chain slightly deviates from the spectrum obtained with the bare subphase and tends to an asymptote at large q_z. Overall, the reflectivity signal decreases progressively upon compression and its value at the asymptote, at large q_z, reduces. This suggests that the PDMAEMA layer is not collapsed on the PS layer, but forms a thick layer with chains protruding in the subphase. At high surface pressure, a weak oscillation at low q_z close to the critical wave vector q_c = 0.17 nm^{-1} is detectable. It could be produced by the PS layer. Indeed, although this subphase is contrast-matched with the PS (SLD 6.5 × 10^{-4} nm^{-2}), the PS layer still contribute to the reflectivity as it is located between the air (SLD 0.0 × 10^{-4} nm^{-2}) and a PDMAEMA layer (SLD 1.6 × 10^{-4} nm^{-2}).

The data collected for the two subphases were fitted simultaneously with the constrain that roughness and thickness for the equivalent layers must have the same values on each subphase. It was always possible to fit the SNR curves on 82%H_2O/18%D_2O subphases with a single layer, but a model containing at least two layers was mandatory to fit the data on 100%D_2O subphase. This shows that all PS blocks are located in the upper layer, which is consistent with the qualitative picture of the monolayer with the PS hydrophobic block adsorbed at the surface and the PDMAEMA block in water corresponding respectively to the upper and lower layer in the model. The fit of the 1-layer in the 82%H_2O/18%D_2O contrast involves four different parameters, the thicknesses and SLD of layer and the roughness of the two interfaces (air/layer and layer/lower layer). It revealed to be however possible to fit the data without roughness for these two interfaces within error bars. This indicates that the roughness remains below 0.3 nm.

As given in Table 2, the thickness of the upper layer at large area per chain (60 nm^2, 40 nm^2 and π = 3 mN m^{-1}) is 0.54 nm, which is in the range of the radius of gyration of the PS_{30} block in a poor solvent (R_{G_PS} = $aN^{1/3}$ = 0.77 nm [17] with a = 0.25 nm [28]). Upon further compression, the thickness of this layer slightly increases at 15 mN m^{-1} and reaches 1.14 nm at 28 mN m^{-1}, suggesting a deformation of the PS layer. The area per chain at which such deformation started, 9 nm^2 per molecule at 15 mN m^{-1}, is however larger than the limit area of the PS monolayer, i.e. about 3 nm^2 per polymer molecule. Considering the PS_{35} homopolymer isotherm, one can reasonably assume that no thickness variation of the monolayer occurs before the lift-off which takes place at 4 nm^2 per molecule.

The progressive increase of the SLD of the upper layer upon compression (see Table 2), while its thickness remains constant, up to 3 mN m^{-1}, agrees with a layer of PS coils becoming denser along the reduction of the available area at the air-water interface. Then, when the thickness of the PS layer increases, at large surface pressure, the SLD becomes constant at 4.5 10^{-4} nm^{-2}. This value is much lower than the one calculated for a PS layer (6.5.10^{-4} nm^{-2}) formed by close packed coils, as expected if the limit area were reached. This result indicates a clear effect of the PDMAEMA blocks that can either prevent the close packing of the PS coils *via* repulsive interactions or partially desorb from the water subphase to locate in this upper layer.

To select which of these two scenarios is most likely to occur, it was necessary to estimate if some PDAEDMA blocks were present in the upper layer. To this aim, we computed the volume fraction occupied by air in such upper layer, Φ_{air}, by means of two different methods:

In the first one, Φ_{air}^{fit} is calculated from the scattering length density ρ_{fitted} used to fit the SNR data, assuming that the layer is composed by only air and PS:

$$\rho_{fitted} = (1 - \Phi_{air}^{fit}) \cdot \rho_{PS}^{melt}, \quad (1)$$

where ρ_{PS}^{melt} is the SLD of a PS melt.

In the second method, $\Phi_{air}^{computed}$ is calculated from the number of deposited polymer molecules and the macroscopic area of the layer:

$$(1 - \Phi_{air}^{computed}) = \frac{V_{ps} \cdot n_{PS}}{t_{PS}^{fitted} \cdot A_c}, \quad (2)$$

Table 2
Upper Part: SLD and thickness of the PS layer obtained from the fits of the neutron reflectivity curves of Fig. 3 at pH = 2. Lower part: volume fraction of air in the first layer upon compression of the monolayer Φ_{air}^{fit} deduced from the SLD resulting from the fit of the neutron reflectivity curve and $\Phi_{air}^{computed}$ calculated from the macroscopic density of the layer.

	60 nm^2	40 nm^2	3 mN m^{-1}	15 mN m^{-1}	28 mN m^{-1}
SLD ($\times 10^{-4}$) nm^{-2}	1.6	2.3	3.8	4.5	4.4
Thickness (nm)	0.54	0.54	0.54	0.80	1.14
Φ_{air}^{fit}	75%	64%	41%	30%	32%
$\Phi_{air}^{computed}$	85%	77%	48%	31%	34%

where n_{PS} is the number of PS blocks deposited (calculated from number of PS-PDMAEMA deposited), t_{PS}^{fitted} the thickness fitted for the first layer, A_c the available area for the molecules at the air-water interface and V_{ps} is the volume of one block in the melt. This volume is calculated from $V_{ps} = M_{PS^d}/\mathcal{N}_A \cdot d_{melt}$ with M_{PS^d} the average molar mass of the PS^d_{30}, d_{melt} the density of a PS melt, and $\mathcal{N}_A$ the Avogadro number. The results of the two methods are gathered in Table 2.

The volume fractions calculated with the two methods are very close, especially at high surface pressure. This observation is in favor of a layer containing only PS and air. The minimum volume fraction of air, about 30% within the layer at the highest surface pressure, can thus be explained as follows: when the PS blocks come close upon compression, they start to interact with each other and contribute to the surface pressure. However, they cannot melt because each block is tethered to one PDMAEMA block that dives into the water. It is then likely that PS coils consequently adopt the conformation of a hemi-spheroid. The compactness of discs in the denser 2D hexagonal packing is 0.9, while it is 0.74 for spheres in the 3D hexagonal structure. However, by considering the PS block as a hemi-spheroid stacked on a planar surface (in a 2D hexagonal packing), the film thickness is above 0.6, leading to a good agreement with the 30% of air in the layer if the PS is slightly deformed by the compression.

In the 100%D_2O subphase, it was possible to fit the data with a two-layers model, keeping fixed all 4 parameters of the upper layer since data for the two subphases were fitted simultaneously. The second layer at the interface with water was then modelled by three parameters: Its thickness, SLD and layer/water roughness. The parameters for the thickness ranged between 9 and 12 nm depending on the pressure. The SLD was very close to the one of the 100%D_2O subphase at low surface pressure and reached a minimal value of $4.9 \cdot 10^{-4}$ nm^{-2}, which corresponds to a PDMAEMEA volume fraction about 27% at the largest probed surface pressure. The layer is thus largely solvated, which is consistent with the situation where the polyelectrolyte chains protrude in the aqueous subphase. However, the roughness obtained from the fit were always in the 7.5 - 9 nm range, which is not physically reasonable when compared with the layer thicknesses. Hence, this two layers model used for data analysis, although well reproducing the data trend, was not satisfactory to describe properly the conformation of the PDMAEMA in water. Thus, we refined the fit of the SNR curves by using another model with a upper layer, associated to the PS, which parameters are fixed to the values of Table 2 and the lower part of the film is sliced in 12 successive layers. The maximum extension of the PDMAEMA brush is theoretically about 20.5 nm. We then described the PDMAEMA layer as a stack of 12 layers with a fixed thickness of 2 nm which leads to a maximum extension of the brush of 24 nm, larger than the theoretical one. This approach allows to consider the dispersity of the layer while limiting the number of free parameters in the model. It also enables to describe a smooth density profile as suggested by the high roughness obtained with the previous two-layers model. In order to constrain the model parameters to converge towards a physical acceptable profile, we imposed the following conditions: (i) all roughness between adjacent layers are set to zero; (ii) Starting from the PS block interface, the solvation of the layers increases continuously from one layer to the next since the PDMAEMA chains are expected to be denser close to the air-water interface and much more loose in the bulk water. Optimization of this model with 12 layers to the experimental data well-reproduced the collected SNR curves.

Fig. 4 shows the profiles of the volume fraction in both blocks within the monolayer as function of depth z, as obtained from the above described model. The PS layer parameters were determined on the 82% H_2O/18%D_2O subphase. For the PDMAEMA layer, the evolution upon compression results in an increase of the density of chains with a maximum fraction of 0.26 of PDMAEMA within the 2 nm from the PS/PDMAEMA interface and at the highest surface pressure. The maximum extension of this polymer is about 25 nm.

Fig. 5 shows schematically the conformation of the chains for pH = 2 at the different surface pressures probed in this study. The performed characterization of the PS-*b*-PDMAEMA copolymer shows that the short PS blocks form a thin layer at low σ with a thickness comparable with their radius of gyration in melt and are well isolated from each other with air in between the blocks. Thus, as expected, the PS blocks localize the copolymer molecules at the air/water interface. At high σ, the

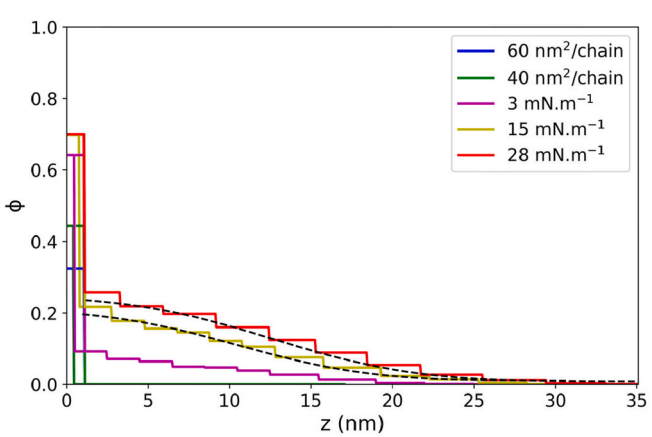

Fig. 4. Fraction of polymer Φ as function of the depth z. The first rectangle starting at z = 0 represents the PS layer, the other ones represent the PDMAEMA layers. The dashed, black line is a fit of the $\Phi(z)$ profile by a Gaussian function.

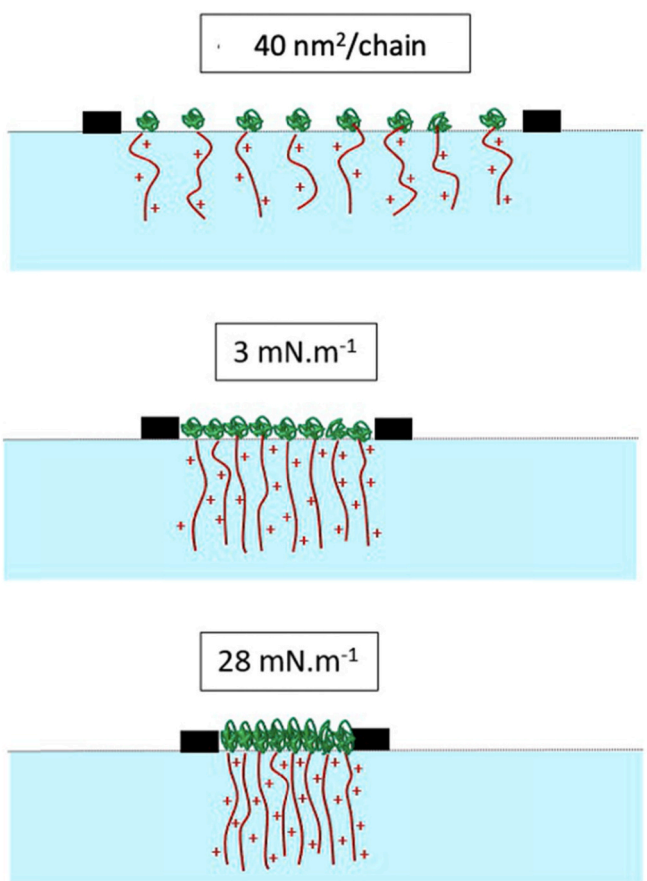

Fig. 5. Schematic representation of the different phases and configurations evidenced on PS-b-PDMAEMA layer at the air-water interface at pH = 2. The PS blocks are in green, the PDMAEMA blocks are in red and the moveable barriers of the Langmuir trough in black.

thickness of such PS layer increases towards larger values than the PS block radius of gyration. However, such increase occurs when the PDMAEMA block protrudes further in the subphase. The molar mass of the PS block is thus sufficiently smaller than the PDMAEMA block to enable the formation of an assembly of PDMAEMA chains at the interface which are not perturbed by the intermolecular interactions between the PS blocks.

On such acidic subphase, the PDMAEMA chains are charged and thus should be in good solvent conditions. Among the theoretically proposed profiles for monomer distributions $\Phi(z)$ as function of depth z, a Gaussian profile characteristic of an osmotic brush has been predicted [32] and experimentally validated for dense polyelectrolyte brush without added salts and in the osmotic regime [29]. It results from the balance between the osmotic pressure in the brush and the elastic force of the chains [11,24,32]. We attempted thus to fit the $\varphi(z)$ profile with such a Gaussian function. The fitted curves are presented in Fig. 4 as a dashed line that well describe the profile obtained from SNR data analysis.

For this pH, we did not observe any transition between a mushroom state and the brush state. Nevertheless, the density at which the mushroom state may occur are too small values to be measured with SNR. In our data, the PDMEAMA layer appears to be in the brush state when the surface pressure is different from zero at low σ.

3.2. *Alkaline subphase*

On the alkaline subphase, the compression isotherm shows a different behavior in Fig. 6 than at pH = 2. For N = 110, the zero-surface pressure plateau extends up to a larger area per chain compared to the acidic subphase, with a lift-off at around 65 nm^2 per chain, followed by an increase of the surface pressure with a compressibility of about 30 m N^{-1}. At about 28 mN m^{-1}, one observes a sloping surface pressure plateau between 20 and 10 nm^2 per chain. A second surface pressure increase region occurs below 10 nm^2 per chain, ending by a collapse at smaller area per chain. The value of the area per chain at the collapse (not presented) is comparable to the one of the acidic subphase, although the collapse pressure is slightly lower. As for the acidic case, PS block does not set the limit areas of the PS-b- PDMEAMA isotherms.

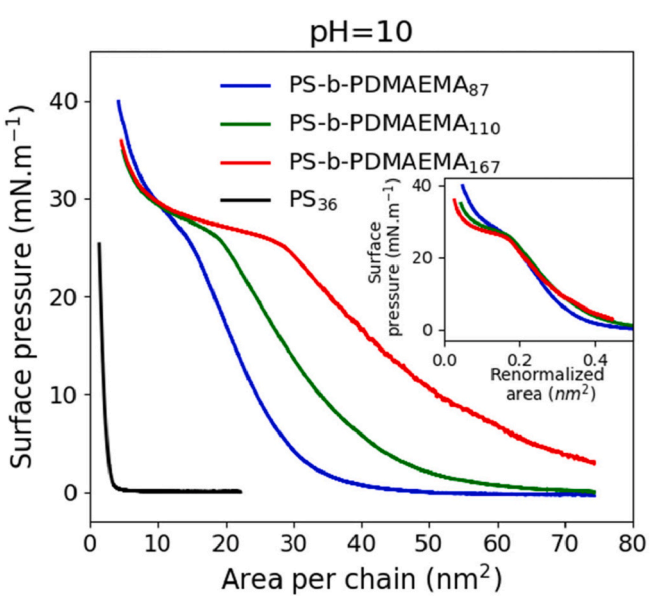

Fig. 6. Surface pressure *vs.* area per chain isotherm of polystyrene homopolymer (PS_{35}) on pure water, PS_{36}-b-$PDMAEMA_N$ with N = 87, 110, and 167 on pH = 10 water subphase at 18 °C. The x-axis is the area per PS-b-PDMAEMA or PS molecule. Inset: Surface pressure *vs.* a renormalized area obtained from area per chain divided by the number of monomers per PDMAEMA block N.

The block length evolution does not change drastically the shape of the π-A isotherms but changes its characteristic values. Increasing the PDMAEMA block length leads to an increase of the lift-off and an extension of the non-zero surface pressure plateau. However, the area per chain and surface pressure of collapse do not change. In order to quantitatively determine the influence of the length of the PDMAEMA block on the surface pressure plateau, we report in the inset of Fig. 6 the surface pressure as function of the area per DMAEMA monomer. This latter shows that the compressibility of the low surface pressure phase remains the same and that the surface density σ, at which the surface pressure plateau starts, scales as N^{-1}. Attempts to scale the data with different exponents (*eg.* 1/2) were unsuccessful. Such isotherm might suggest a mushroom or pancake regime of the copolymer up to 28 m N m^{-1}, followed by a transition to the brush regime at higher surface pressure.

Fig. 7 reports the SNR curves in the $R(q_z)q_z^4$ versus q_z representation of the monolayer of PS^d_{30}-*b*-$PDMAEMA_{100}$ at pH = 10, for both the 82% H_2O/18%D_2O and 100%D_2O subphases. Similarly to the pH = 2 case, the reflectivity of the bare liquid subphases where fitted with the model of a simple rough interface leading to a roughness of about 0.2 nm, and an SLD of $0.72.10^{-4}$ nm^{-2} for the 82%H_2O/18%D_2O subphase and $6.3.10^{-4}$ nm^{-2} for the 100%D_2O subphase.

The data collected for the 82%H_2O/18%D_2O subphase, matching the PDMAEMA block, shows a similar behavior of the monolayer as the one observed on the acid subphase, with an oscillation in the curves of increasing amplitude upon compression of the monolayer. This is thus consistent with a PS layer adsorbed at the air-water interface that becomes denser when the molecular area is decreased. The maximum amplitude of the oscillation in the SNR curves is however less important than observed at pH 2. The area per chain remains sufficiently large along the whole compression isotherm at pH 10 so that the regime where the thickness of the PS coils increases due to steric hindrance is not reached. Under such condition, the size of the coil does not change upon compression. Therefore, the SNR curves were fitted by a single layer of non-interacting PS coils with a constant thickness of 0.56 nm

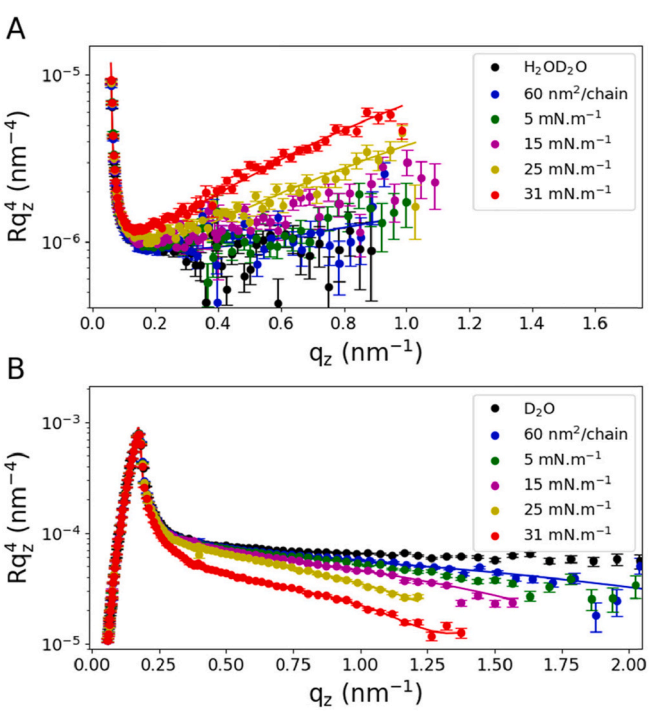

Fig. 7. Neutron reflectometry spectra in Rq_z^4 representation of a PS^d_{30}-b-$PDMAEMA_{100}$ deposited on alkaline pH (pH = 10), 82%H_2O/18%D_2O subphase (A) and 100%D_2O subphase (B). Dots are the experimental points, lines are adjustment with a multilayer model (see text).

and a progressive increase of the SLD up to a volume fraction of PS within the layer of 62% (Fig. 7-A).

On the 100%D_2O subphase matching the PS block, the SNR curve at the largest area per chains is comparable to those of the pure subphase over almost all the q_z range as it deviates from it only at the largest q_z (Fig. 7-B). Such deviation gradually shifts towards the low q_z when the compression is increased up to 25 mN m^{-1}. This indicates the presence of a thin layer at the interface. The evolution of the SNR curves can thus correspond to either a thickening of the layer at constant volume fraction, *ie.* constant SLD, or an increase of the volume fraction, *ie.* increasing SLD, at constant thickness. Discriminating between these two scenarios is in principle very difficult, although both involve an increase of scatterers at the surface. Strikingly, at 31 mN m^{-1}, the SNR curve has a significantly different behavior than for the other surface pressures since it deviates from the Fresnel one over the whole probed q_z range.

A first hypothesis would be that the thin layer evidenced by the SNR curve would correspond to the PS layer. However, in such a case, the contrast of the layer, *ie.* difference in scattering length density with respect to the subphase, should reduce upon compression on the 100% D_2O subphase, as the opposite trend is observed. The only possibility is then that such a thin layer is mostly composed of PDMAEMA blocks adsorbed at the interface in pancake conformation. This interpretation is consistent with the isotherm, since the range of surface pressures where the thin layer is observed on the SNR curves (between 5 mN m^{-1} and 25 mN m^{-1}) corresponds to the regime of the isotherm where the compressibility is constant. At 31 mN m^{-1}, the SNR curve shows the same features at those measured at pH 2, suggesting that the chains are in the brush regime as in acidic case (pH = 2). Interestingly, the change from pancakes to brushes regime occurs between 25 and 31 mN m^{-1}, which is the pressure range of the sloping surface plateau of the isotherm, which could then correspond to the regime of coexistence between brushes and pancakes.

Up to 25 mM m^{-1}, we fitted the experimental data with a two-layers model corresponding to the PS layer and a layer of solvated PDMAEMA with a very small roughness (smaller than 0.3 nm). The parameters for the PS layer were fixed by the values obtained in the 82%H_2O/18%D_2O subphase. For the SNR curve at 31 mM m^{-1}, we used the same model as for the acidic subphases, namely a first layer of 0.56 nm describing the PS layer and 12 additional layers with a fixed thickness of 2 nm to describe the PDMAEMA brush. Fig. 8 presents the volume fraction of polymer as function of the depth z calculated from the SLD values obtained from the fit of the reflectivity curves.

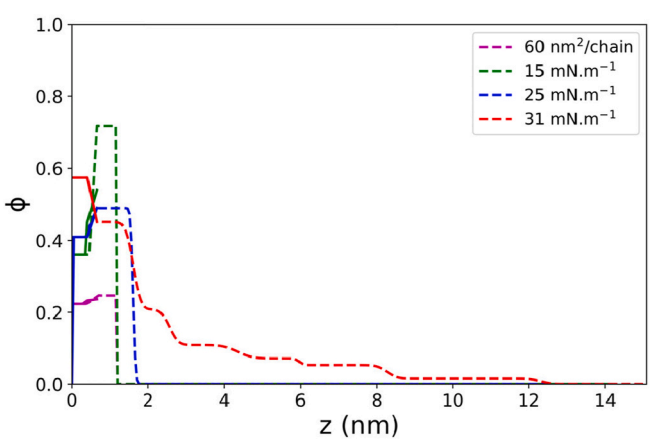

Fig. 8. Fraction of polymer, Φ at depth z in function of the depth obtained after adjustment of the neutron reflectivity curve of Fig. 7 by models with one layer of PS in contact with air and one, two or 12 layers of PDMAEMA in the water subphase depending on the surface density. The continuous line represents the PS layer, the dashed line represents the PDMAEMA layers (5 mN m^{-1} was not represented on the figure since its curve is almost the same that the one at 60 nm^2 per chain).

It exhibits clear-cut differences with the case of the acidic pH since it exhibits only a single homogeneous thin layer at low surface pressures which extends on 0.6 nm with a very small roughness. At 15 mN m^{-1}, the thickness does not change, but the Φ_{DMAEMA} volume fraction reaches a value of 0.7 indicating that the layer is almost no longer solvated. At π = 25 mN m^{-1}, the thickness increased above 1 nm, but the Φ_{DMAEMA} volume fraction decreased, indicating that the blocks start to merge within the subphase. This is the onset of the brush regime. At π = 31 mN m^{-1}, the reflectivity curve is in good agreement with a brush behavior. It has to be noticed than the maximal extension of the brush (~12 nm) remains however smaller than in the acidic case where it extends up to 25 nm.

Fig. 9 shows schematically the conformation of the chains at pH = 10 for different surface pressures. At small density (large area per chain), the PDMAEMA chains form a layer of a few nanometers consistent with chains collapsed near the interface. Above 25 mN m^{-1}, the chains protrude in the subphase as in the brush regime.

In such alkaline subphase, the PDMAEMA chains are uncharged. The hydrophobicity of the chains is increased with respect to the acidic case since the only hydrophilic parts within the PDMAEMA chain are the polar bonds. As a consequence, the affinity of each chain with itself and with the interface is increased. At low σ, polymer chains do not interact with each other and form then pancakes that are distributed evenly on the interface [39,40]. This is consistent with the lift-off of the isotherm (at about 65 nm^2 per chain) that occurs at a much larger area per chain than at pH 2. Indeed, in the pancake regime, the chains occupy a larger part of the interface at low surface density and the critical surface density threshold σ* at which they start to interact occurs at larger area per chain than in the acidic case. The non-zero surface pressure plateau of the isotherm can be attributed to the first order transition from the pancake regime to the brush regime, as usually identified for a pancake –

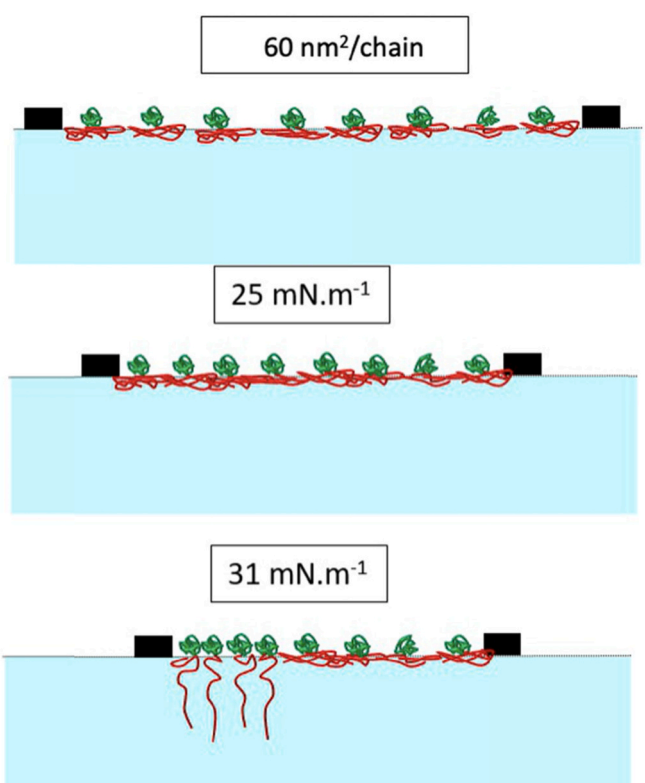

Fig. 9. Schematic representation of the different phases and configurations evidenced on PS-b-PDMAEMA layer at the air-water interface at pH = 10. The PS blocks are in green, the PDMAEMA blocks are in red and the moveable barriers of the Langmuir trough in black.

brush transition where the compression constrains the chains to adopt the brush conformation [39–41].

This situation was theoretically predicted for polymer chains that have a strong affinity with the surface [39,40,42] and observed experimentally with neutral diblock copolymers with a Polyethylene Oxide (PEO) block such as PS – PEO [12,13], neutral triblock copolymers made of Poly(IsoBuylene) (PIB) and PEO [18] but also with polyelectrolytes poly(2-vinylpyridine) (P2VP) grafted layers [43] or PS – Poly-AcrylicAcid (PAA) diblock [17], and even with PDMAEMA grafted on solid substrates [44]. In this latter case, the transition is not induced by the increase of the polymer surface density but by the increase of the PDMAEMA chains length. Most of these studies deal with neutral polymers, which correspond to the case of PS-*b*-PDMAEMA when the PDMAEMA monomers are not ionized in the pH condition where the pancake to brush transition is observed. For neutral polymers, the influence of the length of the chain N on the critical surface density at with the transition occurs σ_t and different values for the exponent for the N-dependence of σ_t have been proposed. From the theory of Alexander [39], Halperin suggested that the transition occurs at $\sim R_F^{-2}$ [41], where R_F is the radius of gyration. In this paper, the authors propose that the density at which the transition starts should scale as $N^{-½}$. According to Ligoure, σ_t should scale as $N^{-0.94}$, with an exponent close to −1 [40]. The difference between the approach of Alexander and Halperin and the one of Ligoure is that the transition occurs at surface coverage larger than the overlapping one [40]. Experimentally Ou-Yang & al measured an exponent of -1 on a triblock copolymer adsorbed on latex spheres in solution [45]. At the air-water interface, Gonçalves da Silva et al. also measured an exponent of 1, on Langmuir monolayers of PS-PEO copolymers but their studies do not include the measurement of the density profile [12]. For the PS-*b*-PDMAEMA un-charged polyelectrolyte, and according to the inset of Fig. 6, the renormalization of the area by N enabled us to have the same value for the onset of the transition. The exponent appears then close to -1 despite the fact that the transition is difficult to determine precisely on the π-A isotherms. These results are therefore in agreement with the model proposed by Ligoure.

4. Conclusion

PS-*b*-PDMAEMA diblock copolymers form stable monolayers at the air-water interface which density can be adjusted through the compression in a Langmuir trough, varying the polymer interaction with itself or with the interface. The behavior of the monolayer strongly varies with the pH subphase, in accordance with the weak poly-base character of the PDMAEMA. At acidic pH, when DMAEMA monomers are fully charged, the brush regime is observed at high densities, where the profile of PDMAEMA blocks follows a Gaussian distribution, as expected for an osmotic brush. At alkaline pH, the PDMAEMA block is neutral and the monolayer exhibits a pancake configuration before undergoing a phase transition to the brush regime upon compression, as identified by a coexistence plateau on the isotherm. We evidenced that the evolution of the surface density at the onset of the transition as function of the PDMAEMA chain length follows a $\nu = -1$ exponent predicted by scaling laws. The PS-*b*-PDMAEMA copolymers chains have thus a rich controlled behavior at the air/water, which provides them a large potential for further applications.

Author contributions

The manuscript was written through contributions of all authors. All authors have given approval to the final version of the manuscript.

Declaration of competing interest

The authors declare that they have no known competing financial interests or personal relationships that could have appeared to influence the work reported in this paper.

Acknowledgment

We thank the Institut Laue Langevin (ILL, Grenoble, France) for providing neutron beamtime (DOI: 10.5291/ILL-DATA.9-11-1788).

References

[1] L. Besnard, M. Protat, F. Malloggi, J. Daillant, F. Cousin, N. Pantoustier, P. Guenoun, P. Perrin, Breaking of the Bancroft rule for multiple emulsions stabilized by a single stimulable polymer, Soft Matter 10 (2014) 7073–7087, https://doi.org/10.1039/C4SM00596A.

[2] L. Besnard, F. Marchal, J.F. Paredes, J. Daillant, N. Pantoustier, P. Perrin, P. Guenoun, Multiple emulsions controlled by stimuli-responsive polymers, Adv. Mater. 25 (2013) 2844–2848, https://doi.org/10.1002/adma.201204496.

[3] V. Bütün, S.P. Armes, N.C. Billingham, Synthesis and aqueous solution properties of near-monodisperse tertiary amine methacrylate homopolymers and diblock copolymers, Polymer 42 (2001) 5993–6008, https://doi.org/10.1016/S0032-3861(01)00066-0.

[4] S.H. Yuk, S.H. Cho, S.H. Lee, pH/Temperature-Responsive Polymer Composed of Poly((*N* , *N* -dimethylamino)ethyl methacrylate- *co* -ethylacrylamide), Macromolecules 30 (1997) 6856–6859, https://doi.org/10.1021/ma970725w.

[5] H. Feil, Y.H. Bae, J. Feijen, S.W. Kim, Mutual influence of pH and temperature on the swelling of ionizable and thermosensitive hydrogels, Macromolecules 25 (1992) 5528–5530, https://doi.org/10.1021/ma00046a063.

[6] L. Bondaz, P. Fontaine, F. Muller, N. Pantoustier, P. Perrin, I. Morfin, M. Goldmann, F. Cousin, Controlled synthesis of gold nanoparticles in copolymers nanomolds by X-ray radiolysis, Langmuir 36 (2020) 6132–6144, https://doi.org/10.1021/acs.langmuir.0c00554.

[7] F. Muller, P. Fontaine, S. Remita, M.-C. Fauré, E. Lacaze, M. Goldmann, Synthesis of nanostructured Metal−Organic films: surface X-ray radiolysis of silver ions using a Langmuir monolayer as a template, Langmuir 20 (2004) 4791–4794, https://doi.org/10.1021/la049534u.

[8] S. Mukherjee, M.-C. Fauré, M. Goldmann, P. Fontaine, Two step formation of metal aggregates by surface X-ray radiolysis under Langmuir monolayers: 2D followed by 3D growth, Beilstein J. Nanotechnol. 6 (2015) 2406–2411, https://doi.org/10.3762/bjnano.6.247.

[9] B. Zhao, W.J. Brittain, Polymer brushes: surface-immobilized macromolecules, Prog. Polym. Sci. 25 (2000) 677–710, https://doi.org/10.1016/S0079-6700(00)00012-5.

[10] H. Ahrens, S. Förster, C.A. Helm, Charged polymer brushes: counterion incorporation and scaling relations, Phys. Rev. Lett. 81 (1998) 4172–4175, https://doi.org/10.1103/PhysRevLett.81.4172.

[11] A. Naji, C. Seidel, R.R. Netz, Theoretical approaches to neutral and charged polymer brushes, in: R. Jordan (Ed.), Surface-Initiated Polymerization II, Springer-Verlag, Berlin/Heidelberg, 2006, pp. 149–183, https://doi.org/10.1007/12_062.

[12] A.M. Gonçalves da Silva, E.J.M. Filipe, J.M.R. d'Oliveira, J.M.G. Martinho, Interfacial behavior of poly(styrene)−Poly(ethylene oxide) diblock copolymer monolayers at the Air−Water interface. Hydrophilic block chain length and temperature influence, Langmuir 12 (1996) 6547–6553, https://doi.org/10.1021/la960604+.

[13] M.C. Fauré, P. Bassereau, L.T. Lee, A. Menelle, C. Lheveder, Phase transitions in monolayers of PS−PEO copolymer at the Air−Water interface, Macromolecules 32 (1999) 8538–8550, https://doi.org/10.1021/ma9900840.

[14] D.E. Gragson, J.M. Jensen, S.M. Baker, Characterization of predominantly hydrophobic poly(styrene)−Poly(ethylene oxide) copolymers at air/water and cyclohexane/water interfaces, Langmuir 15 (1999) 6127–6131, https://doi.org/10.1021/la981461p.

[15] S. Rivillon, M.G. Muñoz, F. Monroy, F. Ortega, R.G. Rubio, Experimental study of the dynamic properties of monolayers of PS−PEO block copolymers: the attractive monomer surface case, Macromolecules 36 (2003) 4068–4077, https://doi.org/10.1021/ma021260z.

[16] R.B. Cheyne, M.G. Moffitt, Novel two-dimensional "ring and chain" morphologies in Langmuir−Blodgett monolayers of PS- *b* -PEO block copolymers: effect of spreading solution concentration on self-assembly at the Air−Water interface, Langmuir 21 (2005) 5453–5460, https://doi.org/10.1021/la0503707.

[17] T.J. Joncheray, S.A. Bernard, R. Matmour, B. Lepoittevin, R.J. El-Khouri, D. Taton, Y. Gnanou, R.S. Duran, Polystyrene- *b* -poly(*tert* -butyl acrylate) and polystyrene- *b* -Poly(acrylic acid) dendrimer-like copolymers: two-dimensional self-assembly at the Air−Water interface, Langmuir 23 (2007) 2531–2538, https://doi.org/10.1021/la062924r.

[18] C. Fuchs, H. Hussain, C. Schwieger, M. Schulz, W.H. Binder, J. Kressler, Molecular arrangement of symmetric and non-symmetric triblock copolymers of poly (ethylene oxide) and poly(isobutylene) at the air/water interface, J. Colloid Interface Sci. 437 (2015) 80–89, https://doi.org/10.1016/j.jcis.2014.09.050.

[19] A. Stocco, K. Tauer, S. Pispas, R. Sigel, Dynamics of amphiphilic diblock copolymers at the air–water interface, J. Colloid Interface Sci. 355 (2011) 172–178, https://doi.org/10.1016/j.jcis.2010.11.049.

[20] H. Matsuoka, S. Nakayama, T. Yamada, X-ray reflectivity study of the effect of ion species on nanostructure and its transition of poly(styrenesulfonate) brush at the air/water interface, Chem. Lett. 41 (2012) 1060–1062, https://doi.org/10.1246/cl.2012.1060.

[21] Z. Guennouni, F. Cousin, M.-C. Fauré, P. Perrin, D. Limagne, O. Konovalov, M. Goldmann, Self-organization of polystyrene- *b* -polyacrylic acid (PS- *b* -PAA) monolayer at the air/water interface: a process driven by the release of the solvent spreading, Langmuir 32 (2016) 1971–1980, https://doi.org/10.1021/acs.langmuir.5b02652.
[22] Z. Guennouni, M. Goldmann, M.-C. Fauré, P. Fontaine, P. Perrin, D. Limagne, F. Cousin, Coupled effects of spreading solvent molecules and electrostatic repulsions on the behavior of PS- *b* -PAA monolayers at the air–water interface, Langmuir 33 (2017) 12525–12534, https://doi.org/10.1021/acs.langmuir.7b02664.
[23] S. Das, M. Banik, G. Chen, S. Sinha, R. Mukherjee, Polyelectrolyte brushes: theory, modelling, synthesis and applications, Soft Matter 11 (2015) 8550–8583, https://doi.org/10.1039/C5SM01962A.
[24] P. Pincus, Colloid stabilization with grafted polyelectrolytes, Macromolecules 24 (1991) 2912–2919, https://doi.org/10.1021/ma00010a043.
[25] J. Yu, N.E. Jackson, X. Xu, Y. Morgenstern, Y. Kaufman, M. Ruths, J.J. de Pablo, M. Tirrell, Multivalent counterions diminish the lubricity of polyelectrolyte brushes, Science 360 (2018) 1434–1438, https://doi.org/10.1126/science.aar5877.
[26] E.B. Zhulina, M. Rubinstein, Lubrication by polyelectrolyte brushes, Macromolecules 47 (2014) 5825–5838, https://doi.org/10.1021/ma500772a.
[27] R. Descas, J.-U. Sommer, A. Blumen, Grafted polymer chains interacting with substrates: computer simulations and scaling, Macromol. Theory Simul. 17 (2008) 429–453, https://doi.org/10.1002/mats.200800046.
[28] H.D. Bijsterbosch, V.O. de Haan, A.W. de Graaf, M. Mellema, F.A.M. Leermakers, M.A.C. Stuart, A.A. van Well, Tethered adsorbing chains: neutron reflectivity and surface pressure of spread diblock copolymer monolayers, Langmuir 11 (1995) 4467–4473, https://doi.org/10.1021/la00011a047.
[29] Y. Mir, P. Auroy, L. Auvray, Density profile of polyelectrolyte brushes, Phys. Rev. Lett. 75 (1995) 2863–2866, https://doi.org/10.1103/PhysRevLett.75.2863.
[30] L. Chen, F. Matsukura, H. Ohno, Direct-current voltages in (Ga,Mn)As structures induced by ferromagnetic resonance, Nat. Commun. 4 (2013) 2055, https://doi.org/10.1038/ncomms3055.
[31] R.R. Netz, D. Andelman, Neutral and charged polymers at interfaces, Phys. Rep. 380 (2003) 1–95, https://doi.org/10.1016/S0370-1573(03)00118-2.
[32] E.B. Zhulina, O.V. Borisov, T.M. Birshtein, Structure of grafted polyelectrolyte layer, J. Phys. II France 2 (1992) 63–74, https://doi.org/10.1051/jp2:1992113.
[33] A. Halperin, Collapse of grafted chains in poor solvents, J. Phys. France. 49 (1988) 547–550, https://doi.org/10.1051/jphys:01988004903054700.
[34] T.P. Russell, X-ray and neutron reflectivity for the investigation of polymers, Mater. Sci. Rep. 5 (1990) 171–271, https://doi.org/10.1016/S0920-2307(05)80002-7.
[35] G.L. Gaines, Insoluble Monolayers at Liquid-Gas Interfaces, Wiley, New York, 1966.
[36] L. Bondaz, Formation de nano-objets métalliques par radiolyse d'ions en présence d'auto-assemblages de polyélectrolytes, PhD Thesis, Sorbonne Université, 2018.
[37] R.A. Campbell, H.P. Wacklin, I. Sutton, R. Cubitt, G. Fragneto, FIGARO: the new horizontal neutron reflectometer at the ILL, Eur. Phys. J. Plus. 126 (2011) 107, https://doi.org/10.1140/epjp/i2011-11107-8.
[38] M. Björck, G. Andersson, GenX : an extensible X-ray reflectivity refinement program utilizing differential evolution, J. Appl. Crystallogr. 40 (2007) 1174–1178, https://doi.org/10.1107/S0021889807045086.
[39] S. Alexander, Adsorption of chain molecules with a polar head a scaling description, J. Phys. France. 38 (1977) 983–987, https://doi.org/10.1051/jphys:01977003808098300.
[40] C. Ligoure, Polymers at interfaces: from a quasi self similar adsorbed layer to a quasi brush first order phase tansition, J. Phys. II France 3 (1993) 1607–1617, https://doi.org/10.1051/jp2:1993221.
[41] A. Halperin, The phase behavior of tethered chains – an overview, J. Macromol. Sci., Part A. 29 (1992) 107–116, https://doi.org/10.1080/10101329208054571.
[42] I. Szleifer, Pancake-to-brush transition in block copolymers, Europhys. Lett. 44 (1998) 721–727, https://doi.org/10.1209/epl/i1998-00531-8.
[43] M.M. Elmahdy, A. Synytska, A. Drechsler, C. Gutsche, P. Uhlmann, M. Stamm, F. Kremer, Forces of interaction between poly(2-vinylpyridine) brushes as measured by optical tweezers, Macromolecules 42 (2009) 9096–9102, https://doi.org/10.1021/ma901567d.
[44] P. Laurent, G. Souharce, J. Duchet-Rumeau, D. Portinha, A. Charlot, 'Pancake' vs. brush-like regime of quaternizable polymer grafts: an efficient tool for nano-templating polyelectrolyte self-assembly, Soft Matter 8 (2012) 715–725, https://doi.org/10.1039/C1SM06362F.
[45] H. Daniel Ou-Yang, Z. Gao, A pancake-to-brush transition in polymer adsorption, J. Phys. II France. 1 (1991) 1375–1385, https://doi.org/10.1051/jp2:1991146.